

Computational and Experimental Analysis of Electromagnetic Fields Induced by RF Coils for High Field Imaging

T. S. Ibrahim¹, C. Mitchel², P. Scmalbrock², D. Chakeres²

¹School of Electrical and Computer Engineering and The OU BioEngineering Center, The University of Oklahoma, Norman, Oklahoma, United States, ²Department of Radiology, The Ohio State University, Columbus, Ohio, United States

Introduction At high magnetic fields (> 3 Tesla), the performance of the RF coil becomes increasingly dependent on its interactions with the human head/body because the human head/body size becomes comparable to the wavelength. Until recently, full-wave numerical methods have seldom been used to model the fields in RF coils for MRI systems. There has not been much need for such an approach because most of the systems are at magnetic field strengths of 1.5 T and below. Thus, circuit approximations are appropriate for modeling RF coils. With the growth in the number of 4 Tesla 7 Tesla and 8 Tesla systems, electromagnetic modeling has become an essential tool for designing and evaluating RF coils in MRI and therefore computational electromagnetic techniques such as the finite difference time domain (FDTD) method [1] have recently flourished [2,3] in modeling RF coils including the birdcage coil and the TEM resonator. It is anticipated that the optimization of RF coils for high field systems will rely heavily upon numerical modeling. In this work, we numerically and experimentally analyze the MR signal. The results show the complexity of the electromagnetic fields and their role in the NMR signal and the effectiveness of the FDTD method when it is applied in a rigorous fashion. The results also demonstrate how applying NMR formulations can produce highly asymmetric inhomogeneous images for symmetrical geometries with linear excitations.

Methods The three-dimensional FDTD model of the TEM resonator consists of 16 coaxial rods. 4.79 mm was used for the spatial step. The coil was numerically tuned by adjusting the gap between the TEM stubs until any of the modes of the TEM resonator is resonant at the desired frequency of operation. The electromagnetic properties of the phantom were assigned according to the Debye theorem [4].

Experiments were conducted using an 8 Tesla whole-body systems. A 16-strut capped TEM resonator loaded with an 18.5 cm sphere filled with 0.5 mM Gd-DTPA to shorten T1 and 0.125 M NaCl for appropriate loading of the coil was used. Sagittal, axial, and coronal gradient echo images of the 18.5 cm sphere (T1 = 370 ms) were acquired using linear excitation and with TR/TE=2000/6.3 ms at 18 flip angles varying between nominal values of 60 and 190° (FOV20 cm). A nominal 90° flip angle was defined for a 1 cm voxel near the isocenter of the phantom using STEAM voxel spectroscopy.

Results And Discussion An experiment was conducted using an 8 T whole-body system. A 16-strut capped TEM resonator loaded with the spherical phantom described above. Fig. 1 displays low flip angle images, measured transmit field, and receive field obtained at 8 Tesla (top row) and their corresponding simulated results obtained at 340 MHz (bottom row) using the FDTD model and the MR signal formulations. The results are shown for mode 0. Excellent agreement is obtained between the experiment and the simulated results in terms of the image, the (transmit) fields. Compared to the experiment, note that the physical location of the excitation source in the simulations differs by a small shift in azimuthal direction. It is expected that with such a phantom size (18.5 cm) and operational frequency (340 MHz), the difference between the distributions of fields will be significant for this experiment. Since low flip angle axial images could be simply approximated by B_1^- and B_1^+ fields. It is expected that the axial images will be symmetric around the source location (Fig.1. (Axial Left)). However as the flip angle increases, the fields can no longer be approximated by B_1^- , times B_1^+ and the semi-mirror symmetry of the B_1^- and B_1^+ fields will be lost due to the presence of the sine function. Consequently, the images will become asymmetric around the source location even for linear excitation. This can be verified from Fig. 2(AXIAL Left) where a high flip angle image is obtained numerically and with experiment. Note that the flip angle was set to 154° in the same voxel for both the experiment and the simulation.

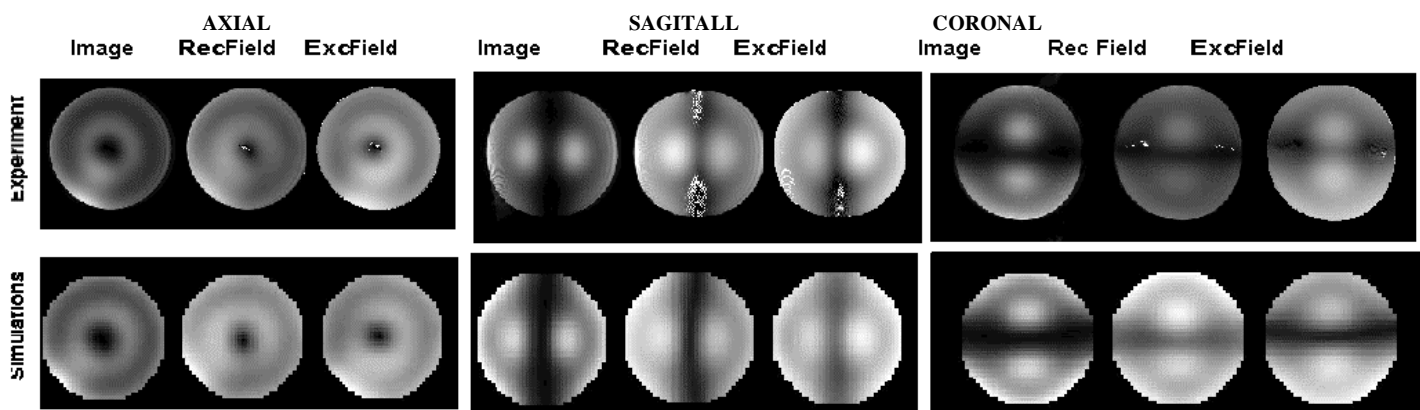


Fig.1: Low flip angle images, extracted transmitt field, and extracted receive field obtained at 8 Tesla and their corresponding simulated results obtained at 340 MHz using the FDTD model. Left set corresponds to axial slices, middle set corresponds to sagittal slices and right set corresponds to coronal slices.

In terms of the coronal and sagittal slices, there is a very interesting point in this case. With the arrangement of the location of the excitation port, 45° from the axis, the mathematics show that in the center of the coil, the B_1^+ field distribution for the coronal slice is equivalent to B_1^+ field distribution of the sagittal slice, and vice versa is also correct. Therefore, both sagittal and coronal low flip angle images are expected to be identical. This can be observed from Fig.1 (Center and Right), the small deviation in the experimental results is due to the fact that there is a small shift in source location. At high flip angles, these images will no longer have the same distribution due to the presence of the sine function as it can be verified in Fig.2 (center and right).

When imaging the head at ultra high field, the distributions of the transmit and receive fields are expected to be different, therefore, it is important to optimize both the transmit and the receive fields to achieve a homogeneous and high signal to noise image.

References:

- [1] K. S. Yee, *IEEE Trans. Ant Prop*, vol. AP-14, no. 4, pp. 302-307, 1966.
- [2] C. M. Collins and M. B. Smith, *Magn. Reson. Med.*, vol. 45, pp. 684-691, 2001.
- [3] T. S. Ibrahim, et al, *Magn. Reson. Imaging*, vol. 19, pp. 219-226, 2001.

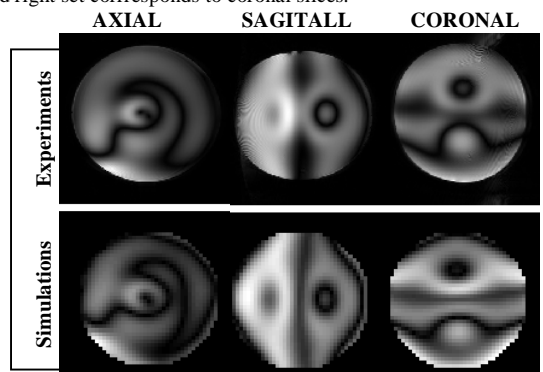


Fig.2 High flip angle images obtained at 8 Tesla and their corresponding simulated results obtained at 340 MHz using the FDTD model. Left set corresponds to axial slices, middle set corresponds to sagittal slices and right set corresponds to coronal slices.